Forward osmosis application of modified TiO_2-polyamide thin film nanocomposite membranes

Maryam Amini, Ahmad Rahimpour*, Mohsen Jahanshahi

*Membrane Research Center, School of Chemical Engineering, Babol University of Technology, Babol, Iran,
Tel./Fax: +98 11 32320342; emails: m.amini.8466@gmail.com (M. Amini), ahmadrahimpour@yahoo.com,
ahmadrahimpour@nit.ac.ir (A. Rahimpour), mjahan@nit.ac.ir (M. Jahanshahi)*

ABSTRACT

Recently, TiO_2 nanoparticles have improved the surface properties and performance of membranes. However, the agglomeration of the nanoparticles remains as one of the major obstacles for generating the uniform surface. One of the best ways to improve dispersion of nanoparticles is the modification of nanoparticles. In this study, chemical modification of TiO_2 was approached using APTES as silane coupling agent. The new thin film nanocomposite (TFN) membranes were synthesized by incorporation of different concentrations of modified TiO_2 nanoparticles in aqueous solution of 1,3-Phenylendiamine (MPD) to enhance the forward osmosis (FO) performance of the membranes. The fabricated TFN membranes were characterized in terms of membranes structure, surface properties, separation properties, FO performance, and compared with common thin-film composite (TFC) membrane. The morphological studies showed that the incorporation of modified TiO_2 significantly changed the surface properties of FO membranes. The TFN membranes exhibited high water permeability and acceptable salt rejection in all ranges of the modified TiO_2 loading (0.01–0.1 wt./v%) in comparison to the TFC membrane. The most permeable membrane, TFN 0.1, had a water flux about 40 L/m^2 h when the active layer facing feed solution. These TFN FO membranes significantly improved the performance of the FO membranes.

Keywords: Modified TiO_2 nanoparticles; Thin-film nanocomposite membrane; Forward osmosis

1. Introduction

The demand of fresh water is a critical challenge faced by humanity today. The membrane separation processes have gained attention as the most promising approach for attending the global water shortage problem [1,2]. A new method for desalination, forward osmosis (FO), is becoming more popular in recent years [1–4]. Since the process does not need hydraulic pressure, it has lower fouling propensity [4,5]. Another advantage for food or pharmaceutical processing is that the process neither demands high temperature nor high pressure [1,6,7]. It also could be used for power generation (applying pressure retarded osmosis process) [8–10].

Generally, FO uses the osmotic pressure differences across the semi-permeable membrane to extract water from a low-osmotic-pressure feed solution to a high-osmotic-pressure draw solution (DS) [1,4,5]. So,

the DS and the membrane have significant roles in FO processes. The main problem of the FO process is internal concentration polarization (ICP) [11–16]. The ICP can cause dramatic loss in the osmotic driving force for water transport, which is different from the external concentration polarization encountered in pressure-driven membrane processes [4,17,18]. In order to minimize the ICP, membranes with low structural parameter (S), relation among thickness, tortuosity, and porosity, are preferred [5]. Therefore, one of the major research topics in the FO area is high performance FO membranes with high water permeability, high salt rejection, and low ICP [2]. Commercial FO membrane, cellulose triacetate flat sheet developed by Hydration technology Inc., has relatively low solute rejection and water flux and can be easily degraded by DS such as ammonium bicarbonate [2,5,19]. Recently, thin-film composite (TFC) FO membranes have demonstrated superior FO water flux and better solute rejection [4,5,20].

Using nanoparticles in the membrane structure has led to the development of membranes with modified properties. Many studies have demonstrated that thin-film nanocomposite (TFN) membranes may significantly improve the membrane properties such as permeability, selectivity, stability, and hydrophilicity in various membrane separation processes [21,22]. Nanoparticles have been used in preparation for membranes for two major purposes. First, producing membranes with desirable structure due to interactions among nanoparticles surface and polymer chains and/or other reactant during membrane preparation. The other aim is the control of membrane fouling caused by nanoparticles functional groups and their hydrophilic properties [23,24].

Titanium oxide (TiO$_2$) is a well-known photocatalytic material, widely used for disinfection and decomposition of organic compounds, and these properties make it interesting as an anti-fouling coating [22]. The main obstacle in using the TiO$_2$ is agglomeration that leads to not only the uneven distribution in the membrane but also potential reduction in anti-fouling abilities of TiO$_2$ particles by changing parameters such as membrane topography and hydrophilicity [25]. So, reducing the agglomeration of TiO$_2$ nanoparticles can influence its ability in the membranes area. There are several methods to avoid agglomeration [26,27], but recently by developing the nanotechnology, incorporation of chemically modified or functionalized nanoparticles has become a topic of great interest. For this purpose, the inorganic particles are coated with organic agents by physical and/or chemical interactions between the particles and organic modifiers. One usual chemical modification

methods is treatment of inorganic particles by silane coupling agents [25,28].

In this research, we modified TiO$_2$ nanoparticles with 3-aminopropyltriethoxysilane (APTES) for chemical modification. The modified TiO$_2$ was dispersed in the aqueous solution of 1,3-Phenylendiamine to prepare the new TFN membranes for FO application. It is worth to note that there is still no exploration of the possibility of FO membranes comprising TiO$_2$ nanoparticles. Subsequently, we explore to characterize the TFN membranes and compared with traditional TFC membranes.

2. Experimental

2.1. Materials

Polysulfone (PSf) (P3500, CAS number: 25135-51-7, Solvay Polymers) as the polymer material for the fabrication of substrates and N,N-dimethylformamide (DMF, >99.5%, CAS number: 4637-24-5, Dae Jung) as the solvent were used for preparing the casting solution. Active monomers were used for synthesis of rejection layer via interfacial polymerization included 1,3-Phenylendiamine (MPD, CAS number: 108-45-2, Merck), triethylamine (TEA, CAS number: 121-44-8, Sigma-Aldrich), n-hexane (>95%, CAS number: 110-54-3, Merck), and trimesoyl chloride (TMC, CAS number: 4422-95-1, Sigma-Aldrich). TiO$_2$ nanoparticles (P25, 20 nm, CAS number: 13463-67-7) were provided by Degussa. Silane coupling agent (3-triethoxysilyl-propylamine, CAS number: 919-30-2) from Merck was used for surface modification of TiO$_2$ nanoparticles. For FO tests, sodium chloride (NaCl > 99.5%, CAS number: 7647-14-5, Merck) was dissolved in DI water and was used as DS.

2.2. Modification of TiO$_2$ nanoparticles

The modification of TiO$_2$ nanoparticles was carried out to decrease the agglomeration and also to increase the stability of the particles in the casting solution [25]. 2.5 g of TiO$_2$ nanoparticles was added to the pure ethanol (25 ml) followed by 30 min sonication in bath. 0.5 g of APTES was added to the solution and stirred for 2 h at 323 k. The separation of particles was down using centrifuging at 10,000 rpm for 10 min. Finally, the TiO$_2$ particles were dried in an oven for 24 h at 323 k [25].

2.3. Preparation of support layer

The PSf membrane substrates were prepared by the phase inversion method [29]. PSf beads (16 wt.%) were dissolved in the DMF at 323 k for at least 5 h until the

solution became homogeneous. In order to casting the solution, the polyester non-woven fabric spread onto the polyester fabric using a homemade casting knife with thickness of 100 μm. Afterwards, the film was immediately immersed in the precipitation bath including DI water, 1 wt./v% SDS, and 2 wt./v% DMF to initiate the phase inversion. The entire composite was allowed to be in the water bath for 20 min followed by washing with DI water for more than 10 h. Finally, the membrane was dried by placing between two sheets of filter paper for 24 h at room temperature.

2.4. Fabrication of polyamide active layer

TFC-FO and TFN-FO membranes were fabricated by interfacial polymerization between MPD and TMC on the surface of PSf substrate. This goal pursued by immersing PSf substrate in the MPD solution (2.0 wt.%) in water containing 2.0 wt.% TEA for 2 min. Next, the membrane was immersed into 0.2 wt.% TMC solution for 30 s to produce interfacial polymerization, resulting in the formation of a thin film of PA in the top layer of PSf support. The resulting composite membranes were subsequently cured in an air-circulation oven at 353 k followed by rinsing and storing in 313 k DI water for at least 5 min. Finally, the membranes were kept in DI water until performing characterization and evaluating membrane performance.

For synthesized of the TFN membranes, the modified TiO_2 was added to the aqueous solution in various concentrations (0.01, 0.05, and 0.1 wt./v%) and were dispersed completely via sonication for 4 h at 303 k followed by 30 min stirring at room temperature. The resultant solution was used as an aqueous solution for interfacial polymerization, which was reacted with organic solution. These synthesized TFN FO membranes are denoted as TFN 0.01, TFN 0.05, and TFN 0.1 assigned to their TiO_2 concentrations.

2.5. Characterization of membranes

The morphological studies of the membranes, cross section, and top surface imaging were observed with a scanning electron microscope (SEM KYKY, EM3200). The membranes surface topology and particle size distribution of nanoparticles were examined using a nanoscope atomic force microscope (AFM model: Easyscan2 Flex).

A contact angle measuring instrument (OCA 15 plus, Dataphysics) was applied to study the hydrophilicity of surfaces of TFC and TFN membranes. The contact angle of probe liquid (DI water) on the surfaces was measured using CCD camera and angle measuring software. To minimize the experimental error, the data reported are the averages of five random locations for each sample [29].

The FTIR spectra of the modified TiO_2 nanoparticles were recorded using a FTIR (Bruker, Model: TENSOR-27) to evaluate the chemical changes of the synthesized FO membranes and modified TiO_2. The wave number range was measured between 5,000 and 400 cm^{-1}. To measure the membrane porosity, a tissue paper was used to blot surface of the wet membranes and remove the excess water from the surface. The wet membranes were weighted (m_{wet}), dried, and reweighted (m_{dry}). Membranes porosity (ε) was obtained by the following equation [4,5]:

$$\varepsilon = \frac{(m_{wet} - m_{dry})/\rho_w}{(m_{wet} - m_{dry})/\rho_w + (m_{dry}/\rho_p)} \times 100 \qquad (1)$$

where ρ_w is the water density and ρ_p is the polymer density.

2.6. Determination of membranes separation properties

Intrinsic separation properties, pure water permeability (A), salt rejection (R), and salt permeability (B) of the synthesized FO membranes were evaluated in a cross flow RO unit according to Ref. [29]. Pure water permeability was determined over an applied pressure of 250 kpa with DI water as feed. The A value was calculated according to [5]:

$$A = \frac{J}{\Delta p} \qquad (2)$$

where ΔP is the applied pressure and J is the permeation flux.

The salt rejection R and salt permeability B were evaluated using 20 mM NaCl feed solution. Rejections were determined using conductivity measurement of both the feed and the permeate:

$$R = \left(1 - \frac{C_p}{C_f}\right) \times 100 \qquad (3)$$

where C_p and C_f are the NaCl concentration in the feed and the permeate, respectively. The salt permeability was calculated from [5,19]:

$$B = \left(\frac{1}{R} - 1\right).J \qquad (4)$$

where J is the RO permeate flux.

2.7. Evaluation of FO performance

The FO performances of the TFC and TFN FO membranes such as water flux and salt permeability were determined in a laboratory-scale FO setup as described in Ref. [29]. The co-current cross flow was fixed in both side of the membrane with the same velocity of 800 ml/min. The feed and DS contained 10 mM NaCl and 2 M NaCl, respectively. The FO water flux J_v was obtained by measuring the weigh change of DS with the digital mass balance:

$$J_v = \frac{\Delta m_{draw}/\rho_{draw}}{A_m \times \Delta t} \tag{5}$$

where ρ_{draw} is the density of DS, A_m is the membrane area, and Δt is the measuring time. The solute flux, J_s, of FO membranes was determined by calculating the volumetric and concentration change of the solutions based on conductivity measurement [5]:

$$J_s = \frac{V_t.C_t - V_0.C_0}{A_m \times \Delta t} \tag{6}$$

where V_0 and V_t are the volumes of feed solution at the beginning and the end of measuring test, respectively, C_0 and C_t are the initial and final salt concentrations of feed solution, respectively.

2.8. Determination membranes structural parameter

According to the classical ICP model developed by Loeb et al. [30], the FO water flux can be determined by the equation which is mentioned below:

$$\text{AL-DS}: \quad J_v = \frac{D}{S}\left[\ln\frac{A\pi_{draw} - J_v + B}{A\pi_{feed} + B}\right] \tag{7}$$

$$\text{AL-FS}: \quad J_v = \frac{D}{S}\left[\ln\frac{A\pi_{draw} + B}{A\pi_{feed} + J_v + B}\right] \tag{8}$$

where D is the solute diffusion coefficient, π_{draw} and π_{feed} are the osmotic pressure of the draw and the feed solution, respectively. The structural parameter, S, can be calculated from these equations (Eqs. (7) and (8)) [5,30].

3. Results and discussions

3.1. TiO₂ nanoparticles modifications

In order to investigate the chemically modified TiO₂, the infrared absorption of TiO₂ nanoparticles was determined. The modification of TiO₂ with APTES is expected to occur by the reaction of surface hydroxyl groups of TiO₂ with the APTES functionalities of silane [25]. Fig. 1 presents the spectra of unmodified and modified TiO₂ nanoparticles. The
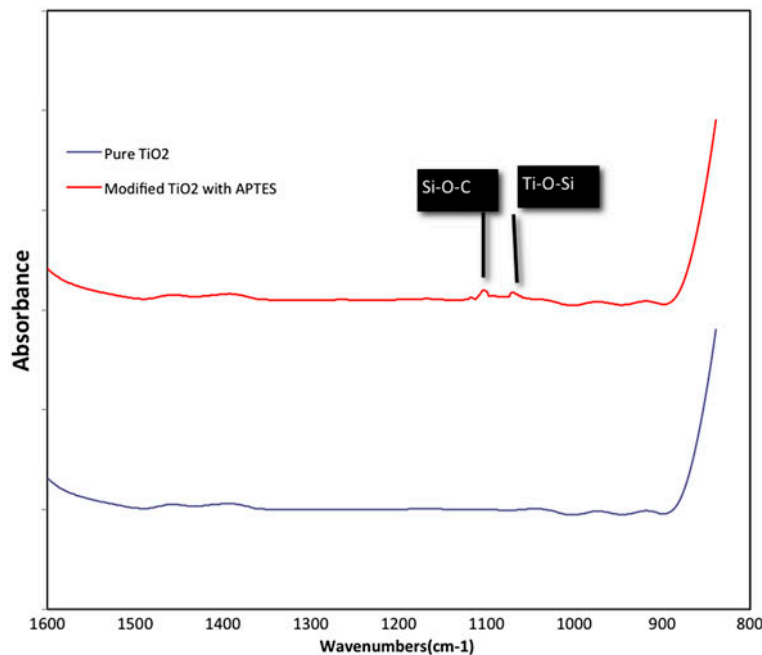

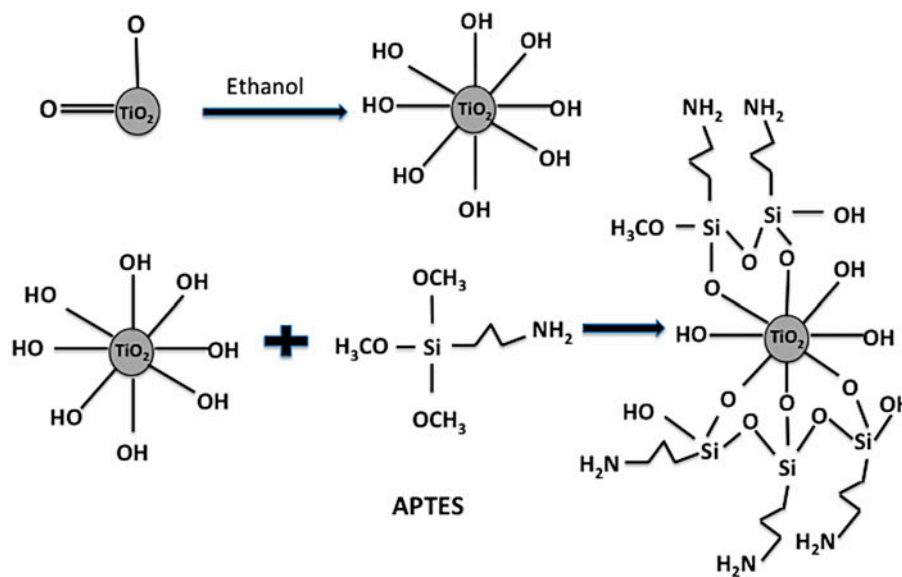Fig. 1. ATR FT-IR spectra of modified TiO₂ with APTES and unmodified TiO₂.

Fig. 2. Functionalization mechanism of TiO$_2$ nanoparticles.

comparison of these two spectra reveals the new double peaks at around 1,132 and 1,080 cm^{-1} that are corresponding to the Si–O–C and Ti–O–Si groups [31,32]. This means that the TiO$_2$ nanoparticles were successfully modified by APTES. The mechanism speculation of chemical functionalization of TiO$_2$ nanoparticles by APTES is shown in Fig. 2.

3.2. FO membranes morphologies

Fig. 3 displays the cross section images of the synthesized FO membranes. The average thickness of the membranes as measured by the micrometer was about 73 ± 5 μm (Fig. 3(a)). The dense skin layer with the thickness of about 600 nm was formed on the top of the support layer that reacts as the rejection layer (Fig. 3(b)). The substrate of this membrane had high porosity with sponge-like structure and small pores in the nanometer ranges. The use of DMF as a solvent without any pore former in the casting solution caused to slow advanced of non-solvent into the polymer solution film. This transition is associated with a small macrovoid and formation of a sponge-like morphology (Fig. 3(b)) [12,33]. It should be noted that some finger-like pores were observed in the support layer that could reduce the structural parameters (S) of the FO membranes [2,34]. The S value is the ratio of the support layer tortuosity and thickness to porosity ($S = l.\tau/\varepsilon$) that is a good indicator of the support resistance to diffusion [12,19]. The PSf substrates tailored in the current study for all TFC and TFN membranes had relatively low S values (about 650 ± 70 μm) that were measured from FO water fluxes.
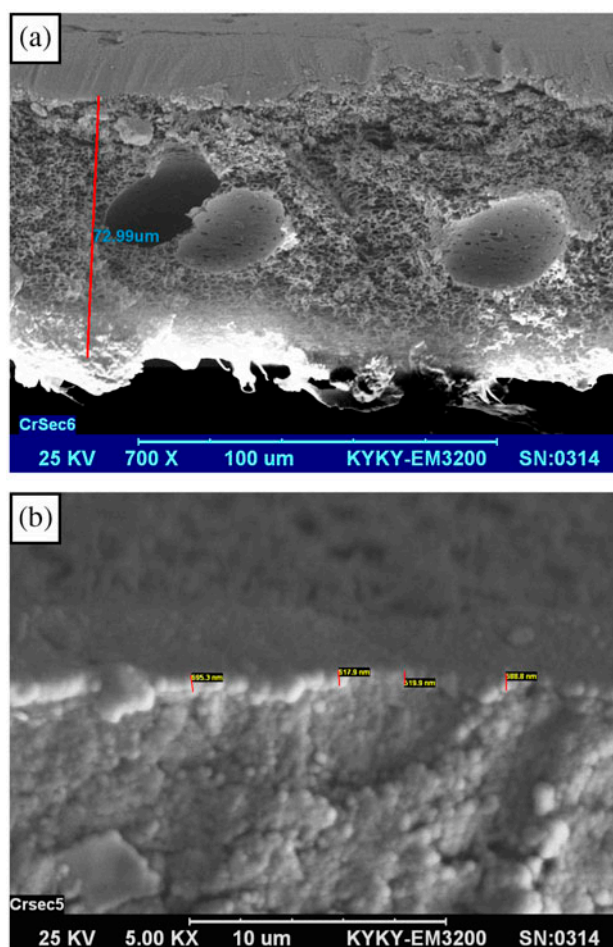

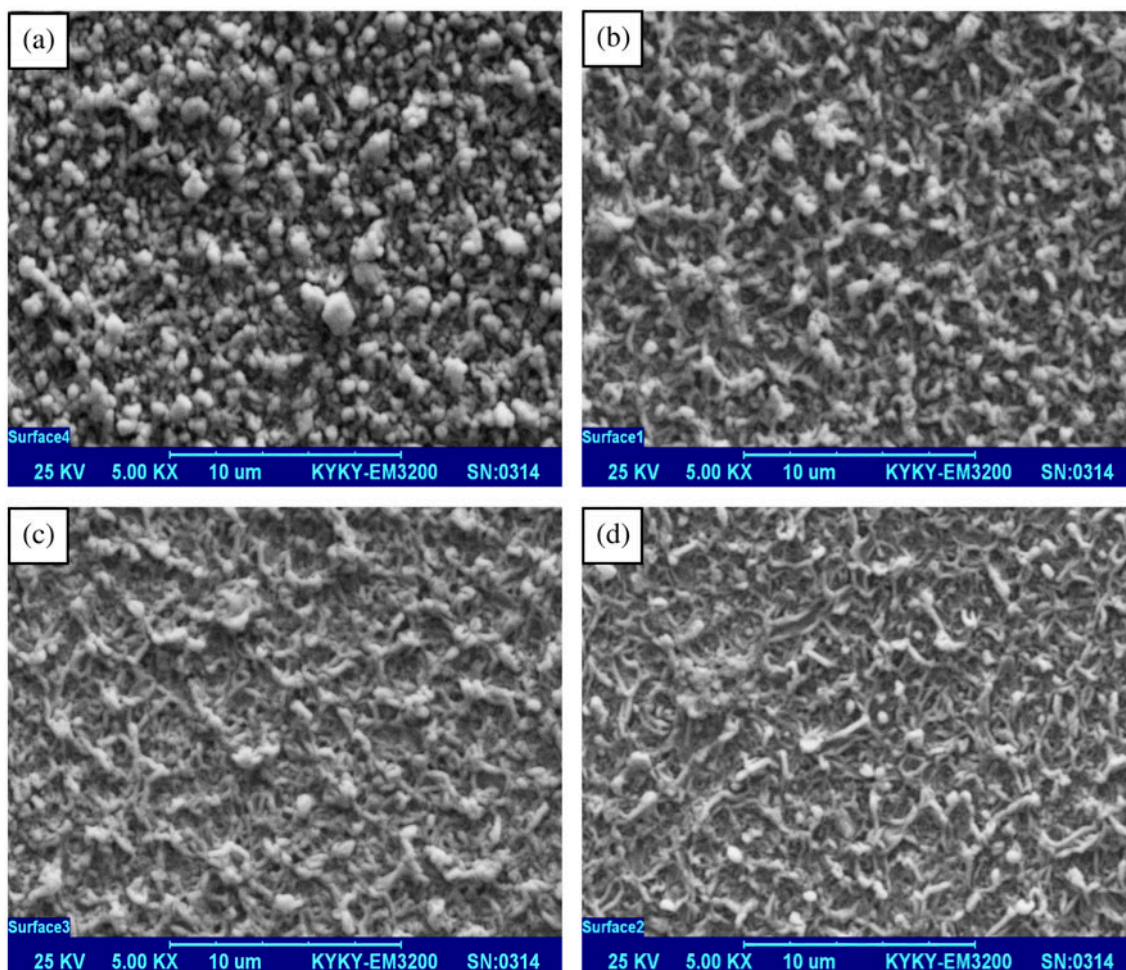Fig. 3. SEM cross-sectional micrographs of TFN 0.01 membrane (a) magnification of 700× and (b) magnification of 5.0 KX.

Fig. 4. SEM micrographs displaying the top surfaces of TFC and TFN FO membranes with different TiO_2 loadings. (a) TFC, (b) TFN 0.01, (c) TFN 0.05, and (d) TFN 0.1.

Furthermore, the top view SEM micrographs of FO membranes with different concentration of modified TiO_2 were shown in Fig. 4. The active rejection layers of the FO membranes were synthesized via interfacial polymerization on the sponge-like skin layer on the PSf substrates. All the TFC and TFN membranes exhibited ridge-valley structures, which is typical for interfacial polymerization with TMC and MPD monomers [5,35]. The observed trend of membranes top surfaces suggests the variation in surface roughness of TFC and TFN membranes. Detailed observation reveals that the incorporation of modified TiO_2 broadened the ridge-valley structure of the FO membranes. Also, the AFM measurements result is in agreement with this structure (Table 1). For instance, the RMS value of TFC (R_a = 112 nm) is sharply decreased compared with that of TFN 0.1 (R_a = 72 nm) as a result of modified TiO_2 loading. Three-dimensional AFM images are shown in Fig. 5. As explained earlier, the

presence of TiO_2 decreased the surface roughness of TFN membranes. The decreased roughness may be attributed to embedded TiO_2 nanoparticles on the surface pores of TFN membranes. On the other hand, the contact angles value of the membranes declined with the increment of the modified TiO_2 loading in the polyamide layer (Table 2). The TiO_2 nanoparticles are highly hydrophilic. Also, the modification of nanoparticles increased the hydrophilic amide

Table 1
Surface roughness parameters of TFC and TFN membranes

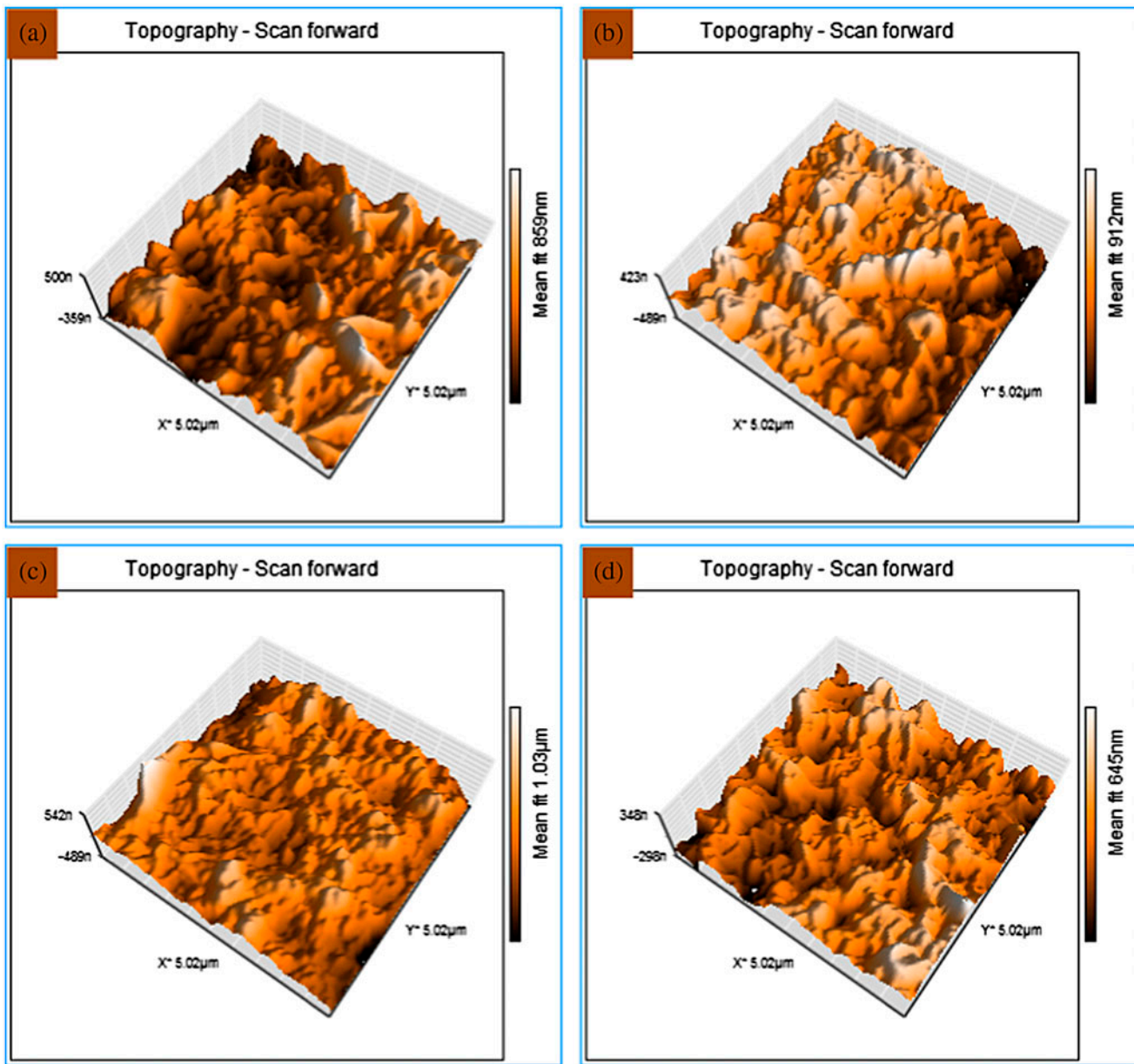| Membranes	S_a (nm)	S_q (nm)	S_z (nm)
TFC	112.48	140	880
TFN 0.01	93	116	790
TFN 0.05	85	108	769
TFN 0. 1	72	89	545

Fig. 5. AFM analyses of (a) TFC, (b) TFN 0.01, (c) TFN 0.05, and (d) TFN 0.1 membranes.

bonds ($-NH_2$) at the surface of membranes. Thus, the incorporation of TiO_2 nanoparticles on the polyamide layer allow the water droplets expanding on it easily [25].

Fig. 6 shows the conceptual model of modified TiO_2 nanoparticles in MPD solution. It is well known that silane coupling agents are first hydrolyzed to silanols and then condensation reactions between the silanols and surface hydroxyl groups on substrate and TiO_2 surface occur [31]. It is supposed that NH_2 groups of APTES also interact with TiO_2 surface,

Table 2
Structural properties of synthesized TFC and TFN FO membranes

Membranes	Porosity[a] (%)	Contact angle (°)
TFC	77 ± 2	66.5 ± 4
TFN 0.0	75 ± 2	62.2 ± 3
TFN 0.05	79 ± 3	52.3 ± 5
TFN 0. 1	81 ± 4	50.5 ± 1

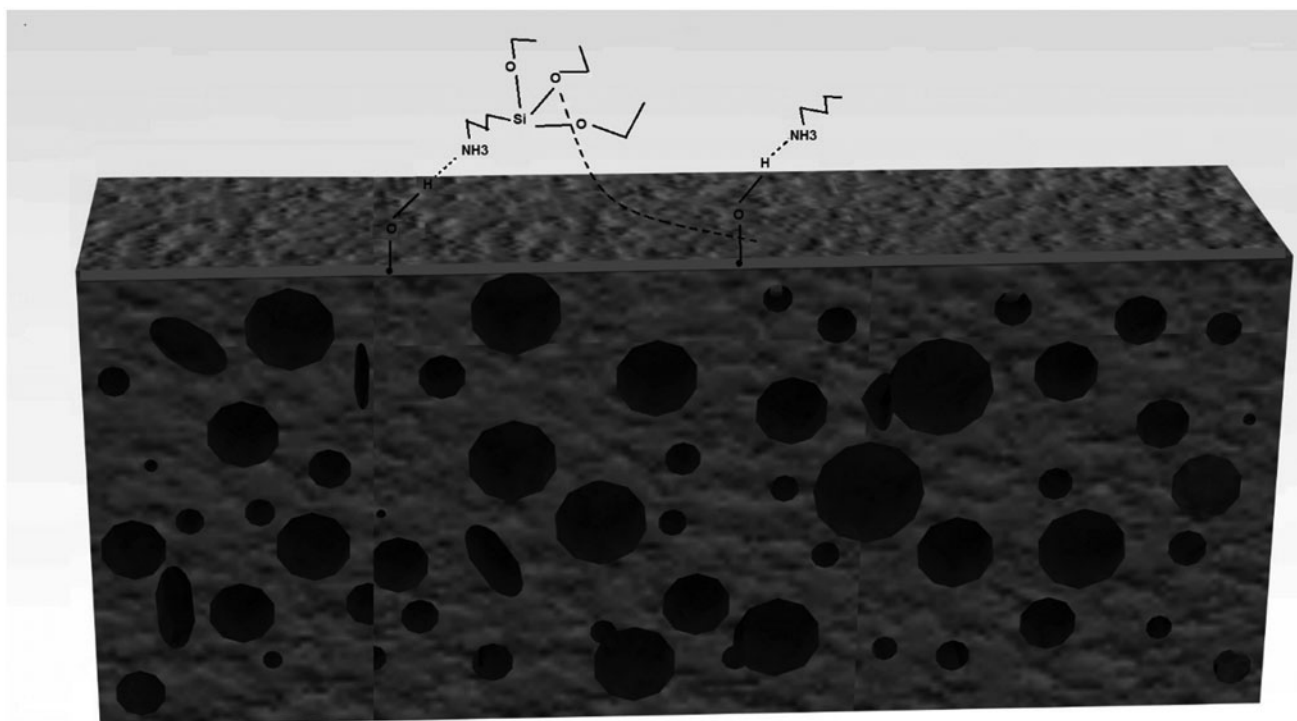[a]Determined by gravimetric measurement and water as a wetting solvent [16].

Fig. 6. Conceptual model of interaction of modified TiO_2 in MPD solution.

Table 3
Separation properties of synthesized FO membrane[a]

Membranes	Pure water permeability[b]		NaCl[c] Rejection (%)	Salt permeability[c] ($\times 10^{-8}$ m/s)	B/A (Kpa)
	(l/m² h bar)	($\times 10^{-12}$ m/s pa)			
TFC	2.93 ± 0.4	8.057 ± 0.2	79	53.5 ± 0.8	67.5 ± 6
TFN 0.01	3.74 ± 0.3	10.28 ± 0.8	81	60.2 ± 1.1	59.6 ± 2
TFN 0.05	3.94 ± 0.2	10.83 ± 0.5	88	36.9 ± 0.4	35.1 ± 4
TFN 0.1	4.6 ± 0.45	12.26 ± 1.3	86	49.9 ± 0.6	41.2 ± 3

[a]All experimental data are reported as the average of at least three repeated measurements.
[b]measured in RO testing mode over an applied pressure of 2.5 bar and DI water as feed solution.
[c]measured in RO testing mode over an applied pressure of 2.5 bar and 20 mM NaCl as feed solution.

which results in higher hydrophilicity. Also, the hydrogen-bonded molecules may self-catalyze the condensation of the silanol with a surface hydroxyl group, and covalent siloxane bond is formed [31]. Therefore, the enhanced hydrophilicity of the TFN membranes surface may be attributed to the amine bonds in the polyamide layer.

3.4. Intrinsic separation properties of synthesized FO membranes

Table 3 presents the separation properties such as water permeability coefficient A, NaCl rejection R, and solute permeability coefficient B of TFC and TFN membranes. Our fabricated TFC-FO membrane had a water permeability of ~8.057×10^{-12} m/s pa, which is in comparable with commercial FO membranes at the same pressure [19]. Also, the TFN-FO membranes had higher water permeability than TFC-FO membrane. For instance, the TFN 0.1 had a pure water permeability of ~12.26×10^{-12} m/s pa with applied pressure of 250 kpa in RO testing mode, which is approximately 52% higher than that of synthesized TFC membranes. Comparison of TFN-FO membranes permeability reveals that incorporation of modified TiO_2 nanoparticles drastically increased separation properties.

Increasing modified TiO$_2$ loading in the TFN-FO membranes improved pure water permeability of the TFN membranes (Fig. 7). For instance, TFN 0.1 had more water permeability of ~12.26 × 10^{-12} m/s pa comparison with TFN 0.05 of ~10.83 × 10^{-12} m/s pa. Such improvement is assigned to the enhanced hydrophilicity of the top layer of the membranes. The salt permeability of the membranes reveals the rejection ability of the membranes. The synthesized FO membranes had relatively low salt permeability due to good rejection ability of the membranes [10]. One of the main factors indicating the selectivity of the FO membranes is the B/A ratio [36]. The *B/A* values of all synthesized TFN-FO membranes were generally smaller than that of TFC and even commercial membranes (in case of TFN 0.05) [19]. This led to lower solute reverse diffusion into the feed water [7,37]. The effect of modified TiO$_2$ concentration on the membrane performance in term of salt rejection has been investigated, as shown in Table 3. In comparison to TFC membrane (79%), TFN 0.01, TFN 0.05, and TFN 0.1 had higher salt rejection (81, 88, and 86%, respectively) at applied pressure of 250 kpa in the RO testing mode. Based on the above findings, synthesized FO membranes exhibited satisfactory salt rejection as well as water permeability.

3.5. Determination of FO performance

Fig. 8 shows the flux of the synthesized FO membranes in both AL-DS (active layer facing DS) and AL-FS (active layer facing feed solution) orientations. The feed and DSs were contained 10 mM and 2 M NaCl, respectively. The higher water flux range (20–41 L/m^2 h) in AL-DS compared to water flux range from 16 to 26 in AL-FS is assigned to the ICP. On the other words, the ICP is more severe in the AL-FS configuration compared to the alternative situation [18,36]. According to Fig. 8, the water flux of TFN 0.01 was 28.4 L/m^2 h in AL-DS, which is significantly higher (41% higher) than that of TFC FO membrane (20.1 L/m^2 h). The enhanced water flux may be attributed to the incorporation of modified TiO$_2$ nanoparticles in the membrane active layer, which may be due to the combination effects of increased porosity and hydrophilicity (Table 2). Moreover, the affinity between hydrophilic functional groups of the modified TiO$_2$ and aqueous media could be improved water permeation (Fig. 8). In addition, the increment of hydrophilicity caused by modified TiO$_2$ nanoparticles is in agreement with such high water flux.

The solute fluxes of FO membranes in both configuration AL-FS and AL-DS are shown in Fig. 9. It should be noted that all synthesized TFN-FO membranes
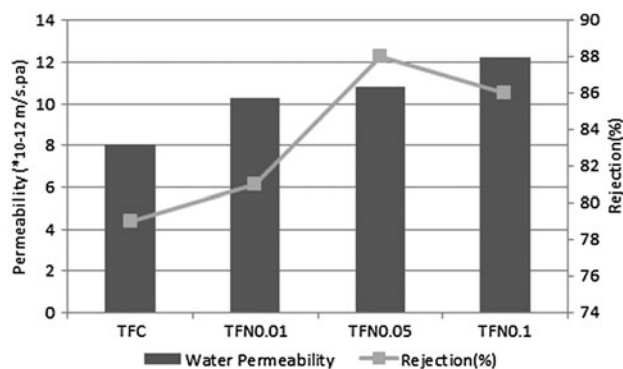

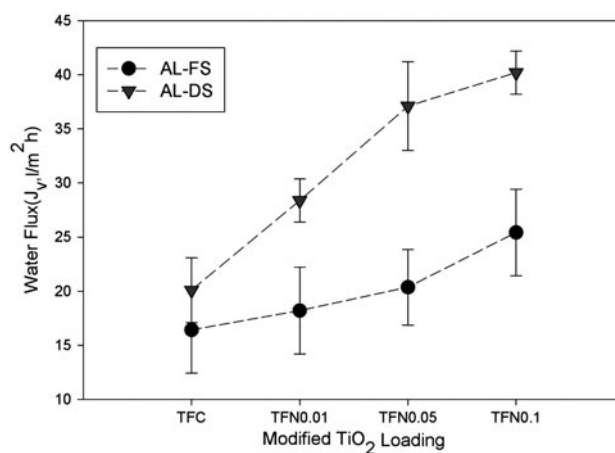Fig. 7. Water permeability and salt rejection of synthesized FO membranes.

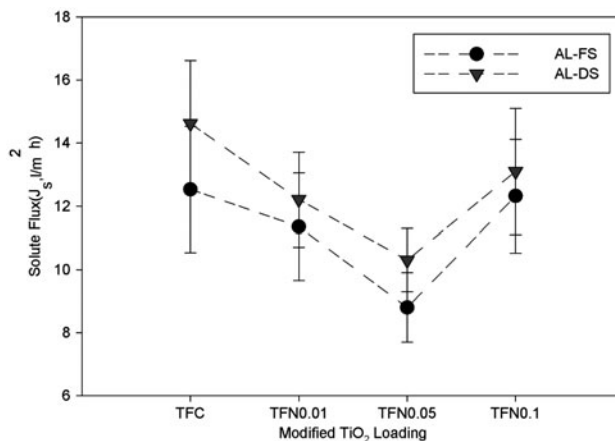Fig. 8. FO water flux of synthesized FO membranes.

Fig. 9. FO solute flux of synthesized FO membranes.

showed lower solute flux in comparison to TFC membranes. The increment of modified TiO_2 loading reduced solute flux. According to the solution-diffusion theory, the solute flux is proportional to the salt rejection coefficient R [19]. On the other words, the higher rejection led to lower solute flux. All synthesized FO membranes have showed excellent FO performance in terms of water flux and solute flux.

4. Conclusions

High performance TFN FO membranes were synthesized in the current study and compared to the synthesized TFC and commercial FO membranes. In order to avoid agglomerations of nanoparticles, commercial TiO_2 powders were modified successfully by chemical modification. Using modified TiO_2 nanoparticles in MPD aqueous solution and incorporation of nanoparticles in the interfacial polymerization improved separation properties and FO performances of membranes. The hydrophilicity of the TFN membranes was increased by incorporation of modified TiO_2 nanoparticles. However, at higher concentrations, the incorporations might affect the interfacial polymerization process and change the selectivity of the membranes. The water flux and solute flux of the FO membranes in both AL-FS and AL-DS mode were enhanced in all synthesized TFN membranes. As the discussed findings, these novel TFN FO membranes have superior possible to FO applications.

Acknowledgments

Nomenclature

A	—	water permeability coefficient (L/m^2 h bar)
A_m	—	effective membrane surface area (m^2)
B	—	salt permeability coefficient (L/m^2 h; m/s)
C_f	—	solute concentration in feed solution (mol/m^3)
C_P	—	solute concentration in permeate solution (mol/m^3)
D	—	solute diffusion coefficient (m^2/s)
D_P	—	polymer density (kg/m^3)
I	—	thickness of membrane(mm)
J	—	pure water flux in RO testing mode(L/m^2 h)
J_s	—	volumetric flux of salt (L/m^2 h)
J_v	—	volumetric flux of water (L/m^2 h)
m_{wet}	—	wet mass of membrane (g)
m_{dry}	—	dry mass of membrane (g)
Δm_{draw}	—	weight change of DS (g)
R	—	salt rejection determined using a feed water containing 20 mM NaCl
Ra	—	mean roughness
S	—	membrane structural parameter (m)
Δt	—	measuring flux time (s)

Greek letters

ε	—	membrane porosity
τ	—	tortuosity
ρ_P	—	polymer density (g/ml)
ρ_w	—	water density (g/ml)
ρ_{draw}	—	density of DS (g/ml)
π_{draw}, π_{feed}	—	osmotic pressures (atm)

References

[1] T.-S. Chung, S. Zhang, K.Y. Wang, J. Su, M.M. Ling, Forward osmosis processes: Yesterday, today and tomorrow, Desalination 287 (2012) 78–81.

[2] S. Chou, L. Shi, R. Wang, C.Y. Tang, C. Qiu, A.G. Fane, Characteristics and potential applications of a novel forward osmosis hollow fiber membrane, Desalination 261 (2010) 365–372.

[3] M.A. Shannon, P.W. Bohn, M. Elimelech, J.G. Georgiadis, B.J. Mariñas, A.M. Mayes, Science and technology for water purification in the coming decades, Nature 452 (2008) 301–310.

[4] G. Han, S. Zhang, X. Li, N. Widjojo, T.-S. Chung, Thin film composite forward osmosis membranes based on polydopamine modified polysulfone substrates with enhancements in both water flux and salt rejection, Chem. Eng. Sci. 80 (2012) 219–231.

[5] J. Wei, C. Qiu, C.Y. Tang, R. Wang, A.G. Fane, Synthesis and characterization of flat-sheet thin film composite forward osmosis membranes, J. Membr. Sci. 372 (2011) 292–302.

[6] K.B. Petrotos, H.N. Lazarides, Osmotic concentration of liquid foods, J. Food Eng. 49 (2001) 201–206.

[7] Q. Yang, K.Y. Wang, T.S. Chung, Dual-layer hollow fibers with enhanced flux as novel forward osmosis membranes for water production, Environ. Sci. Technol. 43 (2009) 2800–2805.

[8] K. Lee, R. Baker, H. Lonsdale, Membranes for power generation by pressure-retarded osmosis, J. Membr. Sci. 8 (1981) 141–171.

[9] K. Gerstandt, K.-V. Peinemann, S.E. Skilhagen, T. Thorsen, T. Holt, Membrane processes in energy supply for an osmotic power plant, Desalination 224 (2008) 64–70.

[10] A. Achilli, T.Y. Cath, A.E. Childress, Power generation with pressure retarded osmosis: An experimental and theoretical investigation, J. Membr. Sci. 343 (2009) 42–52.

[11] J.R. McCutcheon, R.L. McGinnis, M. Elimelech, A novel ammonia—carbon dioxide forward (direct) osmosis desalination process, Desalination 174 (2005) 1–11.

[12] A. Tiraferri, N.Y. Yip, W.A. Phillip, J.D. Schiffman, M. Elimelech, Relating performance of thin-film composite forward osmosis membranes to support layer formation and structure, J. Membr. Sci. 367 (2011) 340–352.

[13] J.E. Cadotte, Interfacially Synthesized Reverse Osmosis Membrane, US petent, US4277344 A, 1981.

[14] N.Y. Yip, A. Tiraferri, W.A. Phillip, J.D. Schiffman, M. Elimelech, High performance thin-film composite forward osmosis membrane, Environ. Sci. Technol. 44 (2010) 3812–3818.

[15] R.L. McGinnis, M. Elimelech, Energy requirements of ammonia–carbon dioxide forward osmosis desalination, Desalination 207 (2007) 370–382.

[16] R. Wang, L. Shi, C.Y. Tang, S. Chou, C. Qiu, A.G. Fane, Characterization of novel forward osmosis hollow fiber membranes, J. Membr. Sci. 355 (2010) 158–167.

[17] X. Song, Z. Liu, D.D. Sun, Nano gives the answer: Breaking the bottleneck of internal concentration polarization with a nanofiber composite forward osmosis membrane for a high water production rate, Adv. Mater. 23 (2011) 3256–3260.

[18] A. Sotto, A. Rashed, R.-X. Zhang, A. Martínez, L. Braken, P. Luis, B. Van der Bruggen, Improved membrane structures for seawater desalination by studying the influence of sublayers, Desalination 287 (2012) 317–325.

[19] N. Ma, J. Wei, R. Liao, C.Y. Tang, Zeolite-polyamide thin film nanocomposite membranes: Towards enhanced performance for forward osmosis, J. Membr. Sci. 405–406 (2012) 149–157.

[20] K.Y. Wang, Q. Yang, T.S. Chung, R. Rajagopalan, Enhanced forward osmosis from chemically modified polybenzimidazole (PBI) nanofiltration hollow fiber membranes with a thin wall, Chem. Eng. Sci. 64 (2009) 1577–1584.

[21] S. Kulprathipanja, Mixed matrix membrane development, Ann. N.Y. Acad. Sci. 984 (2003) 361–369.

[22] K.P. Lee, T.C. Arnot, D. Mattia, A review of reverse osmosis membrane materials for desalination–Development to date and future potential, J. Membr. Sci. 370 (2010) 1–22.

[23] C.J. Kurth, R.L. Burk, Thin Film Membranes with Additives for Forward and Pressure Retarded Osmosis, US petent, US20090272692 A1, 2009.

[24] J. Kim, B. Van der Bruggen, The use of nanoparticles in polymeric and ceramic membrane structures: Review of manufacturing procedures and performance improvement for water treatment, Environ. Pollut. 158 (2010) 2335–2349.

[25] A. Razmjou, J. Mansouri, V. Chen, The effects of mechanical and chemical modification of TiO_2 nanoparticles on the surface chemistry, structure and fouling performance of PES ultrafiltration membranes, J. Membr. Sci. 378 (2011) 73–84.

[26] M.-L. Luo, J.-Q. Zhao, W. Tang, C.-S. Pu, Hydrophilic modification of poly(ether sulfone) ultrafiltration membrane surface by self-assembly of TiO2 nanoparticles, Appl. Surf. Sci. 249 (2005) 76–84.

[27] M.-L. Luo, W. Tang, J.-Q. Zhao, C.-S. Pu, Hydrophilic modification of poly(ether sulfone) used TiO_2 nanoparticles by a sol–gel process, J. Mater. Process. Technol. 172 (2006) 431–436.

[28] V. Gun'ko, E. Voronin, E. Pakhlov, V. Zarko, V. Turov, N. Guzenko, R. Leboda, E. Chibowski, Features of fumed silica coverage with silanes having three or two groups reacting with the surface, Colloids Surf., A 166 (2000) 187–201.

[29] M. Amini, M. Jahanshahi, A. Rahimpour, Synthesis of novel thin film nanocomposite (TFN) forward osmosis membranes using functionalized multi-walled carbon nanotubes, J. Membr. Sci. 435 (2013) 233–241.

[30] S. Loeb, L. Titelman, E. Korngold, J. Freiman, Effect of porous support fabric on osmosis through a Loeb-Sourirajan type asymmetric membrane, J. Membr. Sci. 129 (1997) 243–249.

[31] E. Ukaji, T. Furusawa, M. Sato, N. Suzuki, The effect of surface modification with silane coupling agent on suppressing the photo-catalytic activity of fine TiO_2 particles as inorganic UV filter, Appl. Surf. Sci. 254 (2007) 563–569.

[32] V. Vatanpour, S.S. Madaeni, A.R. Khataee, E. Salehi, S. Zinadini, H.A. Monfared, TiO_2 embedded mixed matrix PES nanocomposite membranes: Influence of different sizes and types of nanoparticles on antifouling and performance, Desalination 292 (2012) 19–29.

[33] P. van de Witte, P. Dijkstra, J. van den Berg, J. Feijen, Phase separation processes in polymer solutions in relation to membrane formation, J. Membr. Sci. 117 (1996) 1–31.

[34] Q. Saren, C.Q. Qiu, C.Y. Tang, Synthesis and characterization of novel forward osmosis membranes based on layer-by-layer assembly, Environ. Sci. Technol. (2011) 5201–5208.

[35] C.Y. Tang, Q.S. Fu, C.S. Criddle, J.O. Leckie, Effect of flux (transmembrane pressure) and membrane properties on fouling and rejection of reverse osmosis and nanofiltration membranes treating perfluorooctane sulfonate containing wastewater, Environ. Sci. Technol. 41 (2007) 2008–2014.

[36] C.Y. Tang, Q. She, W.C.L. Lay, R. Wang, A.G. Fane, Coupled effects of internal concentration polarization and fouling on flux behavior of forward osmosis membranes during humic acid filtration, J. Membr. Sci. 354 (2010) 123–133.

[37] S. Zou, Y. Gu, D. Xiao, C.Y. Tang, The role of physical and chemical parameters on forward osmosis membrane fouling during algae separation, J. Membr. Sci. 366 (2011) 356–362.